Northumbria Research Link

Research

Reverse osmosis and forward osmosis fouling: a comparison

Robert W. Field[1,2] · Qianhong She[3] · Farrukh Arsalan Siddiqui[4] · Anthony G. Fane[5,6]

© The Author(s) 2021   OPEN

Abstract

Our previously reported exploration (Journal of Membrane Science 565 (2018) 241–253) on the differences between fouling in reverse osmosis (RO) and forward osmosis (FO), used alginate as a foulant with initial conditions that ensured that the starting fluxes were the same. That study found that for a cellulose triacetate (CTA) membrane the extent of fouling, based on the analysis of foulant resistance, was greater when the membrane was part of a FO system. Herein, using the same methodology, results for a thin film composite membrane with alginate as the foulant are presented and these confirm the same general conclusion namely that the extent of foulant accumulation in FO mode is more severe than in RO mode. Furthermore the specific fouling resistance with alginate fouling in FO is more than for RO. However examining the overall operation including cleaning as well as fouling, this study suggests that FO operation is potentially less sensitive to fouling phenomena than RO for similar feed materials. This is due to the driving force compensation coming from a changing level of ICP. Some preliminary work including that with silica particles is also reported.

Abbreviations

AL–DS	Active layer facing draw side
AL–FS	Active layer facing feed side
CP	Concentration polarisation
CTA	Cellulose triacetate
DCP	Dilutive concentration polarisation
DS	Draw solution
ECP	External concentration polarisation
FO	Forward osmosis
FS	Feed solution
ICP	Internal concentration polarization
PLC	Programmable logic controller
PRO	Pressure retarded osmosis
RO	Reverse osmosis
TFC	Thin film composite

✉ Robert W. Field, robert.field@northumbria.ac.uk; ✉ Qianhong She, qhshe@ntu.edu.sg | [1]Faculty of Engineering and Environment, Northumbria University, Newcastle NE1 8ST, UK. [2]Department of Engineering Science, University of Oxford, Oxford OX1 3PJ, UK. [3]Singapore Membrane Technology Centre, Nanyang Environment & Water Research Institute, Nanyang Technological University, Singapore, Singapore. [4]Department of Mechanical Engineering, Bahauddin Zakariya University, Multan 60800, Pakistan. [5]School of Chemical and Biomolecular Engineering, The University of Sydney, Sydney, NSW 2006, Australia. [6]UNESCO Centre for Membrane Science and Technology, University of New South Wales, Sydney, NSW 2052, Australia.

Springer

A	Water permeability coefficient (m^3/m^2-Pa)	
B	Solute permeability coefficient (m^3/m^2)	
D	Diffusion coefficient (m^2/s)	
F	Overall net driving force across the active layer of the membrane (Pa)	
F_{dcp}	Concentration polarization factor for DCP (dimensionless)	
F_{ecp}	Concentration polarization factor for ECP (dimensionless)	
J_s	Solute flux (m^3/m^2 s)	
J_w	Water flux (m^3/m^2 s)	
k_{ca}	Mass transfer coefficient for channel adjacent to active layer	
k_{sup}	Mass transfer coefficient within support layer (m/s)	
R_f	Foulant resistance (m^{-1})	
R_g	Universal gas constant (8.3145 m^3 Pa mol^{-1} K^{-1})	
R_m	Hydraulic resistance of the membrane (m^{-1})	
S	Structural parameter (m^{-1})	
T	Temperature (K)	
t	Time	
β	Van't Hoff coefficient	
μ	Fluid viscosity (Pa s)	
η_{rej}	Solute rejection	
π_{ds}	Osmotic pressure of the draw solution (Pa)	
π_f	Osmotic pressure of the feed solution (Pa)	
$\Delta\pi_b$	Osmotic pressure difference between bulk feed and permeate in RO module (Pa)	
ΔP	Applied hydraulic pressure (Pa)	

1 Introduction

From early in the twenty-first century, pressure retarded osmosis (PRO) and forward osmosis (FO) and have received considerable attention [1]. The conceptual simplicity of both processes, and the ambition to have more sustainable processes with a lower carbon footprint, has generated this interest. The former is concerned with power production, and its commercial viability is in doubt with the world's first pilot plant closed and viability being questioned [2, 3]. In closing their pilot plant Statkraft concluded that within the current market outlook the technology could not be sufficiently developed to become competitive "within the foreseeable future" [4]. Herein the concern is with FO which has been considered for varied applications such as desalination [1, 5], and wastewater treatment [6–8]. Unlike PRO, a FO process involves operation at essentially atmospheric pressure for both sides of the membrane. The draw solution (DS) with a higher osmotic pressure on one side of a salt rejecting membrane draws some of the water from an aqueous feed solution (FS) on the other side of the membrane [1]. Unlike pressure-driven reverse osmosis (RO) that is a relatively energy-intensive process, osmotically driven FO process only requires minimum electrical energy for pumping the DS and FS solutions. It has been suggested that a hybrid FO system that incorporates a DS regeneration process may also outperform conventional RO when treating challenging feedwaters (e.g., the feedwater with high salinity or specific challenging contaminants) [9, 10]. However these suggestions regarding outperformance are dependent upon a key assumption regarding the regeneration process, namely that is uses 'waste' heat. This is so because when DS regeneration is required the overall energy balance will not favour FO over RO.

When comparing the performance of FO and RO in practical applications, energy consumption is one of the major factor in the evaluation [9]; the other is fouling and the efficiency of membrane cleaning [6, 7, 9–12]. Our recent paper [11] included a detailed critical review of fouling in FO and RO. The key points are well worth recapitulating. Owing to the different driving forces for FO and RO (i.e. osmotic pressure vs. hydraulic pressure), many researchers had presumed that FO fouling behaviour was different from that of RO and it has often been broadly claimed that osmotically driven FO has a lower fouling tendency and greater fouling reversibility than pressure-driven RO. See [11] for extensive list of references. In addition to our recent findings [11], a number of other studies have reported observations that did not support the view point asserting that FO operation had a lower fouling tendency. For example, Lay et al. [13] did not observe differences in the flux decline between FO and RO fouling and they attributed this to the low initial water flux that was said to be below the critical flux of the system; today this might be better termed threshold flux [14]. Of particular relevance to the present study is the one by Jang et al.

[15] using alginate and silica as the foulants. They observed that fouling propensity was higher for FO compared with both RO and membrane distillation. In an earlier study on alginate and silica fouling for RO under constant flux operation at 40 l/m^{2}hr (well above the critical flux for both foulants), Fane and Chong [16] observed no clear difference in the trans-membrane pressure profiles when the feed pressure was varied from 22 to 30 bar. We concur with the conclusion that this observation suggests that foulant layer resistance (including any compaction) is physically related to the drag force arising from the from water flux (which was the controlled variable) and not the hydraulic pressure per se.

Continuinging the recap of the background presented in [11], it is noted that the inconsistent findings on FO and RO fouling between different groups of researchers have been attributed to two factors. One is the variation in experimental methods used, the other the different analytical approaches [11]. With respect to the present study a few of the earlier observations remain particularly pertinent. The first is that in most of the prior studies, experimental conditions for FO and RO have not been controlled in a comparable manner and furthermore this has not been recognised in the analysis of the data. For RO the apparent driving force across the membrane is typically held constant (i.e., hydraulic pressure, ΔP is maintained constant) whilst for FO the overall nominal driving force (i.e. the osmotic pressure difference between the bulk DS and the bulk FS) has typically decreased gradually due to the DS being gradually diluted whilst the FS becomes gradually concentrated [15, 17–20]. Also in many prior studies the FO water flux was a corrected one that was obtained by combining experimental fouling flux and baseline flux under non-fouling conditions whereas the RO reported flux was the one directly observed from experiments [15, 17–19]. As explained elsewhere, this simple approach does not account for the influence of concentration polarization (CP), especially internal concentration polarization (ICP), upon the driving force [21–23]. Thirdly, the fouling propensity between FO and RO has typically been based on the extent of flux decline [15, 17–20]. However, in both FO and RO, especially FO, the flux decline is not just a reflection of the evolution of foulant accumulation on the membrane, because the flux decline is related both to the change in the overall hydraulic resistance and that in the driving force. The latter is affected by concentration polarisation (CP), both external but also internal concentration polarisation (ICP), which themselves are dependent upon flux. The latter is present in FO, but not RO, and plays a major role in determining the effective driving force in FO as opposed to the nominal one.

Regarding the last point it is instructive to examine the following general membrane equation in which F represents the *net* driving force across the active layer of the membrane and other terms have their normal meaning (as defined in the nomenclature).

$$J_w = F/\mu(R_m + R_f) \tag{1}$$

Rearrangement and differentiation with respect to time yields:

$$\frac{dR_f}{dt} = \frac{1}{\mu J_w}\frac{\partial F}{\partial t} - \frac{F}{\mu J_w^2}\frac{\partial J_w}{\partial t} \tag{2}$$

Regarding the second term on the right hand side, the term $\partial J_w/\partial t$ is negative (flux declines). Thus there is a positive increase in the fouling resistance and often it is only this second term that is considered. However where flux changes lead to a change in the driving force the first term on the right hand side will not be zero. For RO, the driving force is $\Delta P - \Delta\pi_b\exp(\frac{J_w}{k_{ca}})$ and so as flux declines there is a small/modest change in the overall driving force. However for FO the influence of flux upon the overall driving force is much stronger as discussed by Field and Wu [24] and as shown in Figure 6 of [24] which illustrates the huge significance of ICP. A reflection upon the equation for the driving force also serves to make the same point. For FO, in AL-FS orientation, the driving force is:

$$F_{FO} = \left[\pi_{ds}\exp\left(-\frac{J_w}{k_{sup}}\right) - \pi_f\exp\left(\frac{J_w}{k_{ca}}\right)\right] + (B/A)\left[\exp\left(-\frac{J_w}{k_{sup}}\right) - \exp\left(\frac{J_w}{k_{ca}}\right)\right] \tag{3}$$

and for the AL-DS orientation it is:

$$F_{FO} = \left[\pi_{ds}\exp\left(-\frac{J_w}{k_{ca}}\right) - \pi_f\exp\left(\frac{J_w}{k_{sup}}\right)\right] + (B/A)\left[\exp\left(-\frac{J_w}{k_{ca}}\right) - \exp\left(\frac{J_w}{k_{sup}}\right)\right] \tag{4}$$

Given that $k_{sup} \ll k_{ca}$ due to the influence of the support layer the impact of CP upon the driving force is very significant in FO. The importance can be appreciated by noting that for the experiments reported below, the osmotic pressure of the draw solution for the experiments run in FO mode was around a minimum of five times greater than the hydraulic pressure

required to obtain the same flux as for those run in RO mode. The theoretical explanation for this is principally two-fold. Firstly in AL-FS orientation the strength of the FO draw is severely attenuated by the internal concentration polarization within the support layer; the term $\exp\left(-\frac{J_w}{k_{sup}}\right)$ in Eq. (3) is much smaller than unity. Secondly the second term on the righthand side of Eq. (3) is negative. The attenuation of driving forces in forward osmosis due to flux is discussed in more detail elsewhere [24]. Here it is simply noted that there is a very large difference between the nominal driving force ($\pi_{ds} - \pi_f$) and the effective driving force and that this difference is related exponentially to volumetric flux. Given this, it will be readily appreciated that for FO the changes in flux will significantly impact the effective driving force [11, 22, 23]. Overall it is noted that for FO processes, an examination of the decline in flux in isolation does not accurately indicate the evolution of fouling i.e. the evolution of foulant accumulation. Consequently, the same approach to analysis as used in our previous paper [11] will be adopted here to elucidate evolution of fouling resistances and effective driving force for RO and FO.

2 Materials and methods

2.1 Chemicals and membranes

All of the chemicals used in this study were of analytical grade, unless otherwise stated. Ultrapure deionised (DI) water, which was supplied by a Milli-Q Ultrapure water system (Millipore Singapore Pte Ltd) with a resistivity of 18.2 MΩ cm, was used in the preparation of all solutions. In both FO and RO fouling experiments the base feed solution comprised 45 mM NaCl + 5 mM CaCl$_2$ and was prepared in a quantity of 5 L. The colloidal silica (Sigma-Aldrich) had a particle size of 50 nm to 200 nm and a surface area of 140 m^2/g (as per information from supplier). Experiments with colloidal silica as the foulant were prepared at a concentration of 2000 mg of silica per litre. The other model foulant was the sodium salt of alginic acid (alginate, Sigma-Aldrich St. Louis, MO) and these solutions were prepared with a concentration of 200 mg/L alginate.

The membranes used during the experiments were provided by Hydration Technologies (Albany, OR). One was cellulose-tri-acetate (CTA) while the other was a polyamide thin film composite (TFC). Being proprietary, the detailed membrane chemistry is unknown, but both comprised a dense selective layer and a porous support layer. These membranes were used in both FO and RO experimental tests. The CTA membrane comprising a dense selective layer and a porous support layer embedded within a polyester woven mesh fabric has been widely used as a model membrane to compare fouling in FO and RO [17, 18, 25].

2.2 FO and RO membrane fouling experiments

The same experimental setup was used for FO and RO experimental tests with only slight modification between the two different test modes; details of the apparatus are given in [11]. This setup has also been used in our previous osmotic membrane fouling experiments and benefits, *inter alia*, from being able to maintain a constant draw concentration [26]. For the FO experiments, a PLC control system monitored the conductivity and hence concentration of the draw solution and the feed solution. The concentration of the former was maintained constant by dosing with a more concentrated NaCl solution whilst the feed was dosed with DI water as required. For the RO experiments there was manual intervention to ensure constant feed pressure and the permeate water was returned manually to the feed side roughly every half an hour so as to maintain the molarity of the feed as essentially constant. These measures ensured that the apparent driving forces for both RO and FO (i.e., the applied hydraulic pressure for RO and the osmotic pressure difference between the bulk DS and the bulk FS for FO) were maintained constant for each experiment. This addressed a deficiency of earlier approaches that was noted in the Introduction.

The operating pressure for RO and the draw solution concentration for FO were chosen to give essentially the same initial water flux to provide similar initial fouling environments. The setup had a PLC control system that allowed automatic data acquisition. For FO tests, both FS and DS were recirculated with Hydra-Cell positive displacement diaphragm pumps. The FO membrane test cell (CF042, Sterlitech Corporation) comprised two symmetric Delrin half-cells (top cell and bottom cell) with identical dimension of flow channel (85 mm length × 39 mm width × 2.3 mm height). Diamond spacers were fixed in the draw channel. The crossflow velocity of the feed solution was set at 7.4 cm/s, while at the draw side it was 20.4 cm/s. At the conclusion of each fouling test, the fouled membrane was either cleaned via surface flushing to investigate the fouling reversibility, or autopsied to determine the foulant deposition. During membrane flushing,

feed solution was replaced with deionised water and cross-flow velocity was increased to 29.6 cm/s. This cleaning session was run for 30 min.

For RO tests, only FS was recirculated, while the permeate water was collected directly in a permeate tank. There was dosing of the feed with DI water to ensure concentration was kept constant. The RO membrane test cell had the same FS flow channel as that for FO. The permeate channel was filled with sintered porous metal plate (with ~ 20 µm mean pore size) that could fully support the membrane against deformation in the RO test. To estimate the rejection, the feed and permeate conductivity were monitored.

The foulant mass load (i.e., amount of foulant deposited on unit area of membrane surface) was determined by foulant extraction followed by measurement of the total organic carbon using a similar protocol reported elsewhere [23] and was briefly summarized in the Supporting Information in [11].

2.3 Determination of foulant resistance for fouled membranes in FO and RO

Before the determination of the foulant resistance on the fouled membranes (R_f), the clean membrane resistance (R_m) was first measured via a RO test using a foulant-free feed solution with the same background electrolyte used for the fouling test. Details are to be found in [11, 27]. The approach taken allows for external concentration polarization (ECP) with the feed channel mass transfer coefficient k_{ecp} being estimated following the approach reported elsewhere [28].

For FO operation the determination of the structural parameter (S) is essential, and this was determined in essentially the same way as in [11]. The two differences from the approach taken in [11] are that herein the membrane rejection was assumed to be 100% in RO mode and the calculation of the foulant resistance (R_f) did not include any allowance for cake-enhanced concentration polarization. The foulant resistance (R_f) on the FO fouled membrane was calculated from π_{ds}, π_{fs}, the experimentally obtained parameters that are time invariant (R_m and S) and those that evolve with time ($J_{w,f}$, $J_{s,f}/J_{w,f}$) using as its basis the osmotic-resistance filtration model expounded by She et al. [23]. Thus for RO:

$$J_{w,f} = \frac{\Delta P - \eta_{rej,f}\pi_f exp\left(\frac{J_{w,f}}{k_{ca}}\right)}{\mu\left(R_m + R_f\right)} \tag{5}$$

The term $\eta_{rej,f}$ is essentially the same as the reflection coefficient, σ, because it is close to unity. The subscript 'f' indicates a fouled condition.

The R_f on the fouled FO membrane was calculated from:

$$J_{w,f} = \frac{(\pi_{ds} - \pi_f) - F_{ecp}\left(\pi_f + \frac{J_{s,f}}{J_{w,f}}\beta R_g T\right) - F_{dcp}\left(\pi_{ds} + \frac{J_{s,f}}{J_{w,f}}\beta R_g T\right)}{\mu\left(R_m + R_f\right)} \tag{6}$$

where the external concentration polarization (ECP) factor, F_{ecp}, at the feed side and dilutive concentration polarization (DCP) factor, F_{dcp}, at the draw side are expressed by Eq. (7) and Eq. (8), respectively.

$$F_{ecp,f} = exp\left(\frac{J_{w,f}}{k_{ca}}\right) - 1 \tag{7}$$

$$F_{dcp} = 1 - exp\left(-\frac{J_{w,f}}{k_{dcp}}\right) = 1 - exp\left(-\frac{J_{w,f}}{D/S}\right) \tag{8}$$

Equation (6) incorporates the effect of reverse solute diffusion (i.e., J_s/J_w), internal concentration polarization (included in F_{dcp}), and external concentration polarization (included in F_{ecp}). Given that these equations allow for the effect of concentration polarisation through modifications to the driving force, the foulant resistance (R_f) term does not include any so-called CP resistance; to do so would be to double count the effect of CP.

The test conditions of the experiments with alginate as foulant are listed in Table 1.

The scouting experiments were with silica using both CTA and TFC membranes and with alginate using the CTA membrane. At the beginning of Sect. 3 there is a brief summary of the results using silica whilst the CTA membrane results using alginate can be found in the Appendix 1. Our definitive results for this combination have been reported in

Table 1 Test conditions for baseline and fouling tests with membrane orientation of active layer facing the feed side. All feed solutions contained 45 mM NaCl + 5 mM CaCl$_2$ with alginate (200 mg/L) as foulant in fouling tests

Test No	Process	Membrane	Driving force	Baseline Test duration	Fouling Test duration	Crossflow velocity of feed solution (cm/s)	Crossflow velocity of draw solution (cm/s)
1	FO	CTA	Draw solution of 2 M NaCl	50 min	1100 min	7.4	11.1
2	FO	CTA	Draw solution of 2 M NaCl	40 min	1000 min	7.4	11.1
3	FO	TFC	Draw solution of 3 M NaCl	50 min	1200 min	7.4	11.1
4	FO	TFC	Draw solution of 3 M NaCl	85 min	1200 min	7.4	11.1
5	FO	TFC	Draw solution of 3 M NaCl	30 min	1450 min	7.4	11.1
6	RO	CTA	19.4 bar hydraulic pressure on feed	70 min	1200 min	7.4	–
7	RO	CTA	18.8 bar hydraulic pressure on feed	30 min	270 min	7.4	–
8	RO	CTA	18.5 bar hydraulic pressure on feed	30 min	270 min	7.4	–
9	RO	CTA	16.5 bar hydraulic pressure on feed	50 min	1050 min	7.4	–
10	RO	TFC	7.0 bar hydraulic pressure on feed	50 min	270 min	7.4	–
11	RO	TFC	7.1 bar hydraulic pressure on feed	30 min	270 min	7.4	–
12	RO	TFC	7.3 bar hydraulic pressure on feed	50 min	1200 min	7.4	–

our earlier paper [11]. The results for RO runs 6–7 and 10–11 (Table 1) have been excluded from further analysis herein as the objective was to make a comparison of fouling under Reverse Osmosis and Forward Osmosis operation over an extended run time starting from the same initial flux and with under constant driving force. Thus the results reported below are based upon runs where the conditions were stable for 1000 + mins.

3 Results and discussion

3.1 Experiments with silica as the foulant

With a 3 M NaCl draw solution neither the CTA nor the TFC membrane fouled—see Fig. 1. It was concluded that the flux generated was insufficient to form a deposit. The CTA membrane could be operated at a hydraulic pressure of 27.5 bar in RO mode and it was found that this was sufficient to generate some initial fouling—see Fig. 2. It was concluded that these observations could be related to the fact that the critical flux [29] was greater than 25 LMH and this value could not be exceeded in the FO experiments but could be exceeded in the RO run.

3.2 Experiments with TFC membrane and alginate as foulant

Baseline tests without the addition of any foulant were performed before each fouling test. The results (not shown here) indicated a near constant flux for both FO and RO in the range 17.7 to 18.1 LMH. Thus for all runs, both FO and RO, the initial flux of operation was ~ 18 LMH.

Figures 3 shows the water flux behaviour during FO and RO fouling tests. For both CTA and TFC membranes the behaviour followed a similar trend. The flux decline was more pronounced in the first 8 h and tended to be much milder later, approaching a limiting flux. At the end of 16 h, the water flux had declined by ~ 50% for RO and around 30% for FO. It is emphasized that this is data for flux decline and because of the evolution of the driving force it is not directly indicative of the evolution of the fouling resistance. This can be readily understood by re-examining Eq. (2) which can be written as:

Fig. 1 Variation in flux with time using CTA and TFC membranes for forward osmosis experiment (ALFS orientation) with feed solution (45 mM NaCl solution + 5 mM CaCl$_2$) with colloidal silica (2 g/L) as foulant and draw solution 3 M NaCl. Crossflow velocity of draw solution set at 14.9 cm/s and of feed solution at 7.4 cm/s
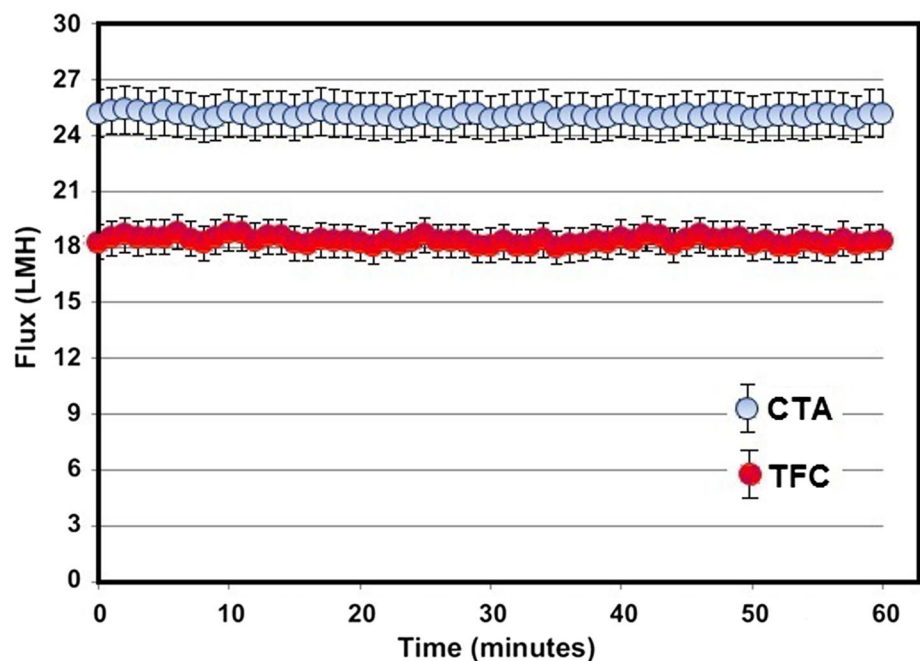
Fig. 2 Variation in flux with time using CTA membrane for reverse osmosis experiment (ALFS orientation) with feed solution (45 mM NaCl + 5 mM CaCl$_2$) with colloidal silica (2 g/L) as foulant and 27.5 bar hydraulic pressure on feed side. Crossflow velocity of feed was set at 7.4 cm/s
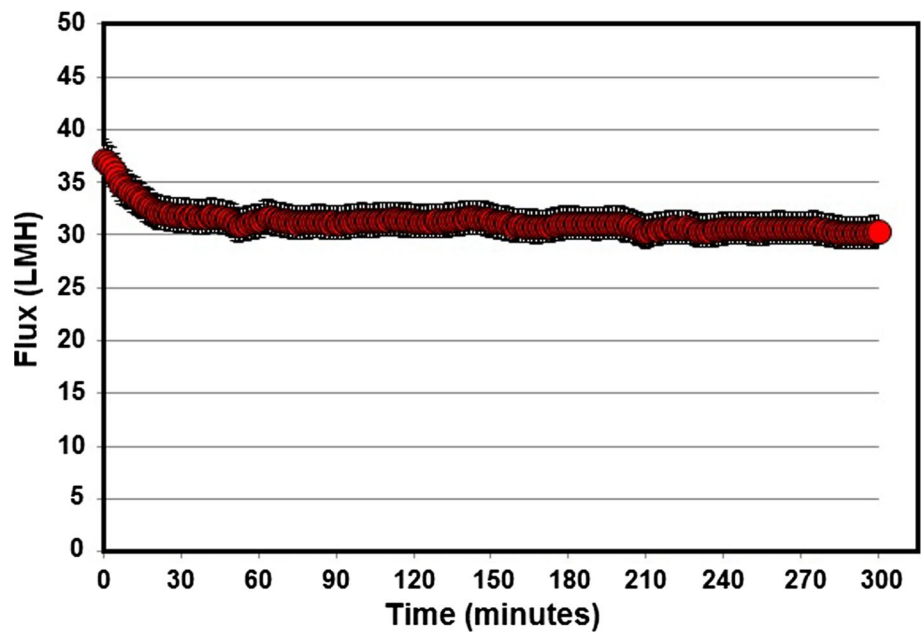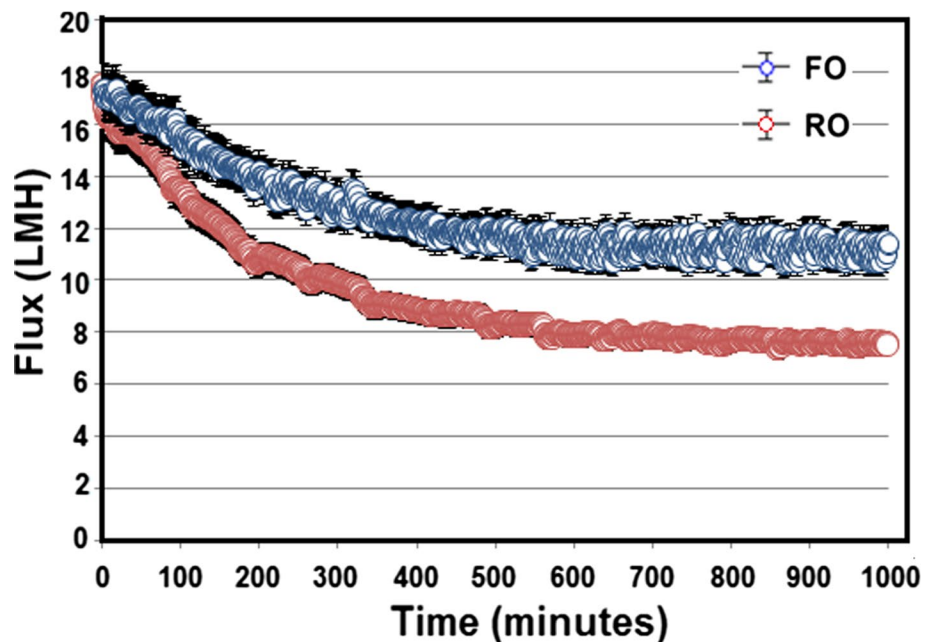

Fig. 3 Comparison of FO and RO performance during membrane fouling using TFC membrane for forward and reverse osmosis experiments (ALFS orientation) with feed solution (45 mM NaCl + 5 mM CaCl$_2$) with alginate (200 mg/L) as foulant for variation in water flux with time

$$\frac{dR_f}{dt} = \frac{F}{\mu J_w}\left[\frac{1}{F}\frac{\partial F}{\partial t} - \frac{1}{J_w}\frac{\partial J_w}{\partial t}\right]$$

(9)

As indicated by Eq. (9), the rate of change of foulant resistance is proportional to the *sum* of the fractional change in driving force and the fractional change in flux. As flux declines both terms are positive for the processes analysed herein. Quantitatively the term $\frac{1}{F}\frac{\partial F}{\partial t}$ is significance in the case of FO, and this will be expanded upon in Sect. 3.3.

After the physical cleaning, water fluxes for both FO and RO recovered significantly: see Fig. 4. The degree of reversibility for FO may have been somewhat overestimated by the headline figures indicated; please take note of the error bars. As deionized water was used during the cleaning phase, near pure water will have been left in the support layer of the membrane. Therefore upon the resumption of FO operation the level of ICP would have been lower than its pseudo steady state value and consequentially there would have been an initial increase in the effective driving force. In retrospect a little more time should have been allowed for the evaluation of flux recovery after physical membrane cleaning.

Fig. 4 Comparison of FO and RO performance during membrane fouling using TFC membrane for forward and reverse osmosis experiments (ALFS orientation) with feed solution (45 mM NaCl + 5 mM CaCl$_2$) with alginate (200 mg/L) as foulant for water flux recovery after membrane cleaning
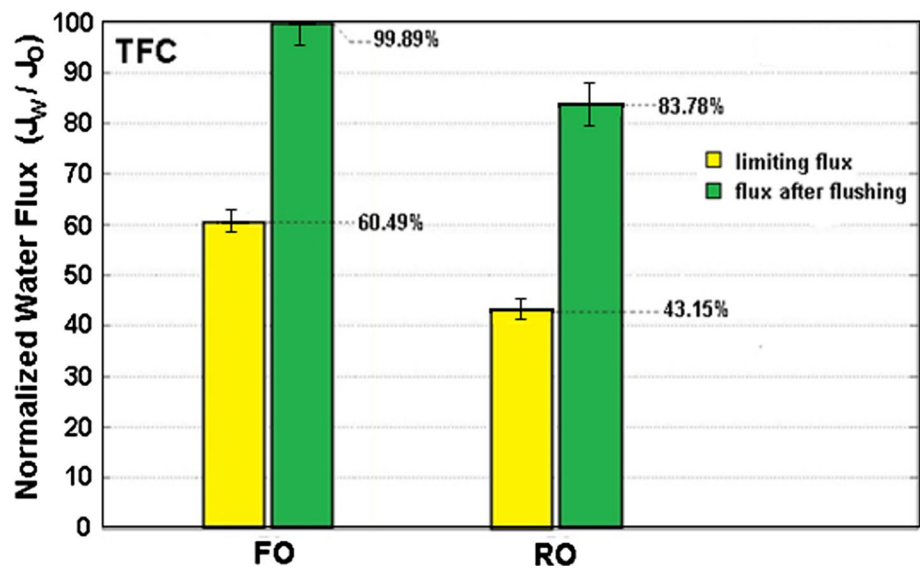
Additional observations are can be found in the Appendix 1 which compares the CTA results therein with CTA results reported previously. As a final observation, it is noted that previous researchers may have taken a similar experimental approach and consequently over-estimated flux recovery after FO operation.

3.3 Analysis of evolution of foulant resistance

A recap of some of the operating conditions will indicate how large the *nominal* driving force was for the FO tests in comparison with that for the RO runs. For the FO test with the CTA membrane the draw solution was 2 M NaCl i.e. equivalent to 99.1 bar [30] whilst in the equivalent RO test (achieving the same flux) the hydraulic pressure on feed solution was 17.7 bar. For TFC membrane tests, the draw solution was 3 M (equivalent to 148.6 bar) and applied hydraulic pressure in RO was 7.6 bar.

As explained earlier the fouling not only reduces the flux but also leads to an increase in the *actual* driving force especially so in the case of the FO runs. This change is known as the ICP self-compensation effect; lower flux reduces ICP and thus the actual difference in osmotic pressure across the active layer of the membrane increases [22]. This point was signaled in general terms in Eq. (9). This showed that when the fractional change in driving force is significant this can have a greater impact upon the calculated increase in resistance than the other term concerned with the decline in flux. For RO, the driving force is $\Delta P - \Delta\pi_b \exp(\frac{J_w}{k_{ca}})$ and so as flux declines there is a small change in the overall driving force. It is small because the magnitude of $\Delta\pi_b$ is small and the exponential term is not particularly large. By contrast the effective driving force for FO changes markedly. Examining the term $\left[\pi_{ds}\exp\left(-\frac{J_w}{k_{sup}}\right) - \pi_f\exp\left(\frac{J_w}{k_{ca}}\right)\right]$ it will be noted that π_{ds} is much larger than the corresponding term for RO and that $k_{sup} \ll k_{ca}$. Thus the exponential term $\exp\left(-\frac{J_w}{k_{sup}}\right)$ changes significantly as flux declines, and consequentially the change in $\pi_{ds}\exp\left(-\frac{J_w}{k_{sup}}\right)$ is large. Hence the magnitude of the term $\left[\pi_{ds}\exp\left(-\frac{J_w}{k_{sup}}\right) - \pi_f\exp\left(\frac{J_w}{k_{ca}}\right)\right]$ will change considerably. The effect is known as the ICP self-compensation effect because the term $\exp\left(-\frac{J_w}{k_{sup}}\right)$ reflects the degree of ICP and as the extent of ICP moderates the effective driving force increases.

The outcome from the calculations, made using Eqs. (5) to (8), indicate that the resistance generated during the FO runs is greater than that generated during the RO runs. This accords with [11]. The results are illustrated in Fig. 5.

After hydraulic cleaning the residual resistances are similar in both pairwise comparisons *i.e.* between RO and FO and between the two types of membrane used. See Fig. 6 for the TFC results.

Confirmation that there was greater deposition on the FO membrane at the end of the fouling runs was obtained by determining the mass of foulant deposition by membrane autopsy. This is reported as a specific deposition mass (amount per unit area) in Fig. 7a whilst Fig. 7b gives the results for the specific resistance (i.e. the resistance per unit mass). All four values of the specific resistance (Fig. 7b) are superficially to some extent similar, but upon closer inspection it will be noted for the TFC membrane that the value for FO is around 2.5 times greater. This accords with the result in [11] for

Fig. 5 Comparison of foulant resistance for FO and RO experiments using TFC membrane (ALFS orientation) with feed solution (45 mM NaCl + 5 mM CaCl$_2$) with alginate (200 mg/L) as foulant
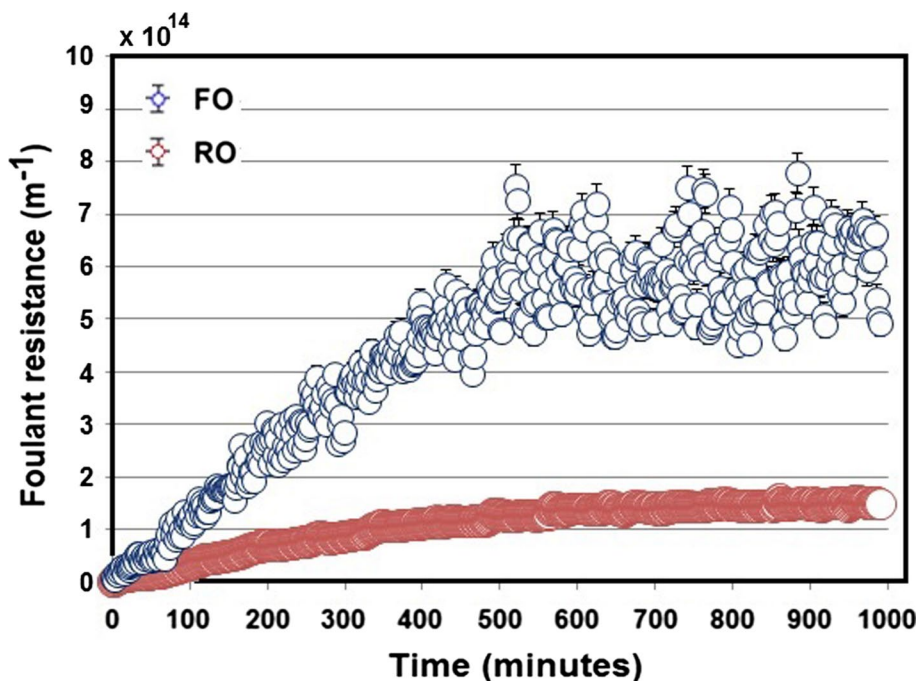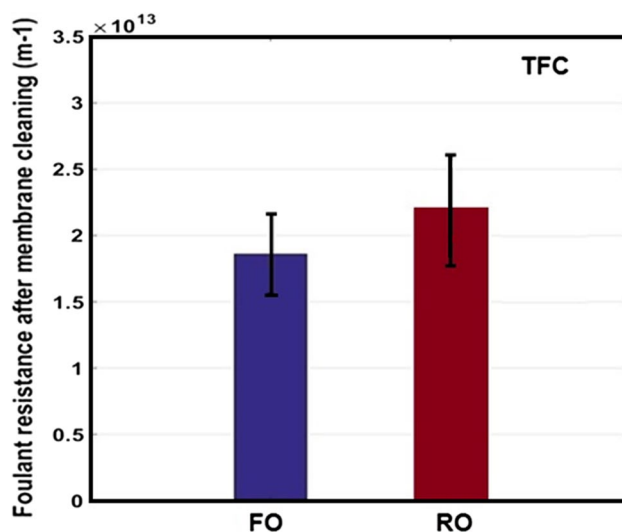

Fig. 6 Comparison of foulant resistance R$_f$ after membrane cleaning in forward and reverse osmosis experiments (ALFS orientation) using TFC membrane


the CTA membrane where we showed that the specific resistance for FO was significantly greater than for RO. Regarding the specific resistance value for CTA in FO mode, it is very close to the one in our earlier work [11].

Regarding the general finding that the specific resistance found with alginate fouling is greater under FO conditions than under RO operation, it is noted that the explanation could be the different ionic gradients for RO and FO at similar fluxes, due to reverse solute diffusion that naturally arises in the case of FO. We have discussed this and other potential reasons for the greater specific resistance in the case of FO previously [11].

4 Concluding remarks

Colloidal silica was replaced with alginate for the later experiments and this foulant was found to have an appropriately low value of critical flux and this enabled the differences in membrane fouling between FO and RO to be explored under comparably controlled experimental conditions. A detailed study with sodium alginate as the foulant and with a CTA membrane has been previous reported by us [7]. Herein the focus is upon results for a TFC membrane. For both membranes it was found that the decline in flux during both FO and RO fouling tests followed broadly the same trend.

Fig. 7 Comparative analysis of forward and reverse osmosis experiments (ALFS orientation) for CTA and TFC membranes using alginate (200 mg/L) as foulant in feed solution of 45 mM Nacl + 5 mM of CaCl$_2$ with application of suitable driving force in each case. **a** Foulant deposition density, m_f **b** Specific foulant resistance
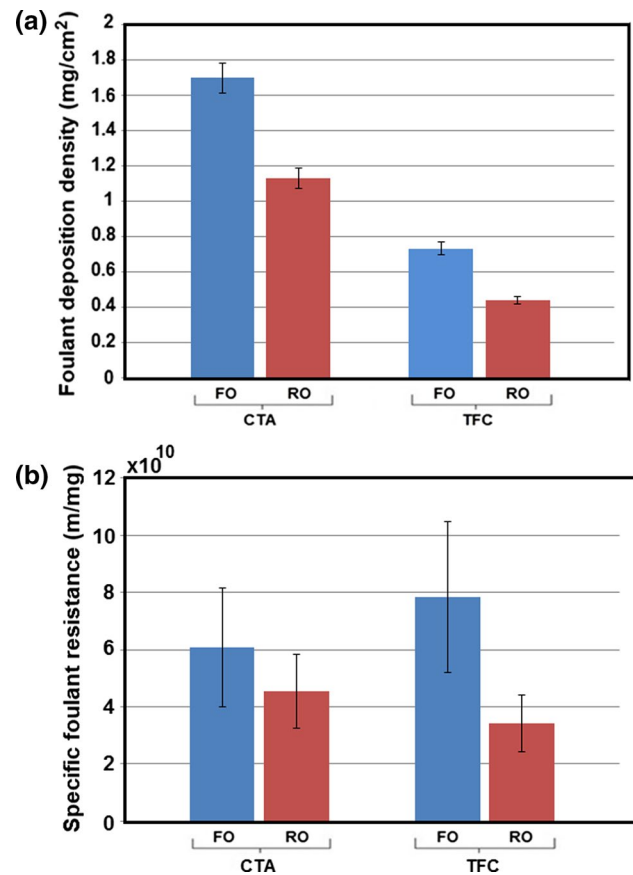
However, the influence of concentration polarization upon the driving force in FO is so pronounced that even modest declines in flux cause a significantly different evolution in the FO driving force compared with the evolution in RO. As the driving forces of FO and RO respond differently to the progression of fouling, care is required when determining the evolution of the foulant resistance. This is especially so for FO.

Membrane autopsy after the fouling tests showed that for both CTA and TFC membranes more foulant had been deposited on the FO fouled membrane than the RO fouled membrane. Herein the specific foulant resistance on the TFC membrane was greater for FO than for RO which accords with the earlier finding for CTA [11]. Taken together it can be concluded that (1) there is no reason to assert that FO operation leads to less fouling than RO operation under comparable starting fluxes, and (2) the specific fouling resistance for FO is not less than for RO. However this study also indicates that FO operation is potentially less sensitive to fouling phenomena than RO for similar feed materials, thanks to the driving force compensation coming from a changing level of ICP. The magnitude of this benefit is likely to be dependent on membrane characteristics (structure factor S) and feed properties.

Authors' contributions AGF and RWF developed the original hypothesis and QS developed the software for the experimental apparatus and analysis. FAS undertook the experiments and prepared the figures. RWF wrote the manuscript and revised it critically together with AGF and QS. All authors read and approved the final manuscript.

Data availability The datasets generated during and/or analysed during the current study are available from the corresponding author on reasonable request.

Declarations

Competing interests The authors declare no competing interests.

Appendix 1

Data for CTA membrane with alginate as foulant

Our definitive results for the combination of CTA and alginate have been reported in our earlier paper [11]. However as these results were obtained at a similar time to the TFC results they are worthy of placing on record. The data on flux decline and recovery are given in Fig. 8.

The results in Fig. 8 for RO are comparable with those we reported earlier [11]. Specifically for CTA membrane the earlier finding was that after physical cleaning, the water fluxes recovered to values of ~ 94% for FO and ~ 96% for RO.

Fig. 8 Comparison of FO and RO performance during membrane fouling using CTA membrane for forward and reverse osmosis experiments (ALFS orientation) with feed solution (45 mM NaCl + 5 mM CaCl$_2$) with alginate (200 mg/L) as foulant. Top: variation in water flux with time Bottom: water flux recovery after membrane cleaning
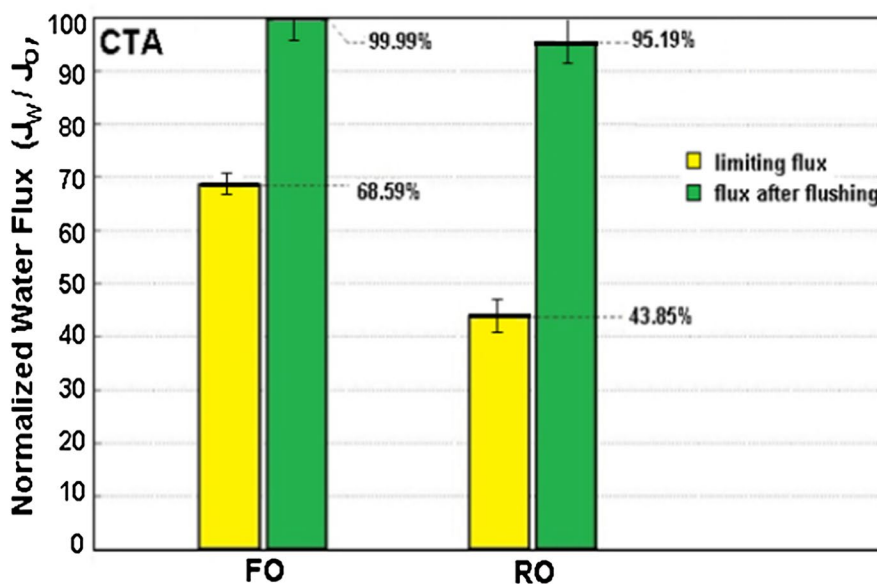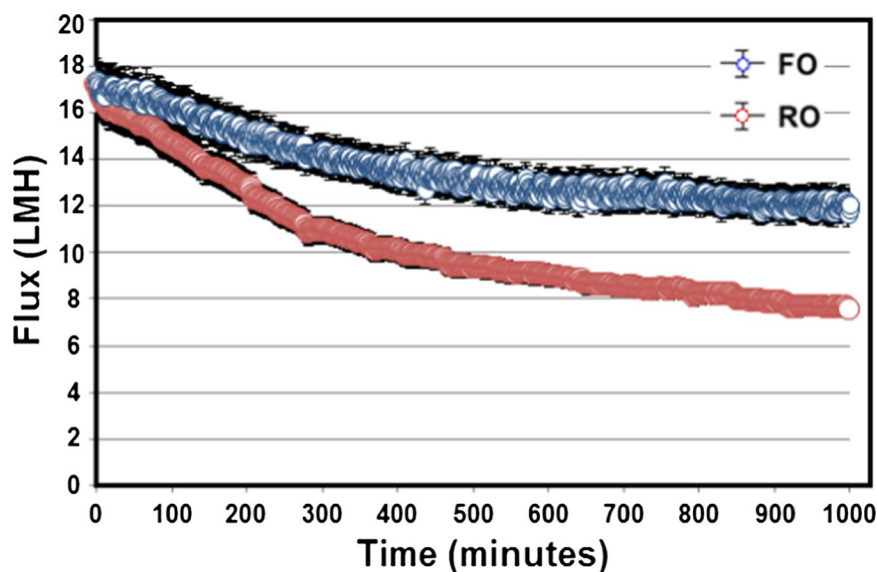
Fig. 9 Comparison of foulant resistance Rf after membrane cleaning in forward and reverse osmosis experiments using CTA membrane (ALFS orientation)
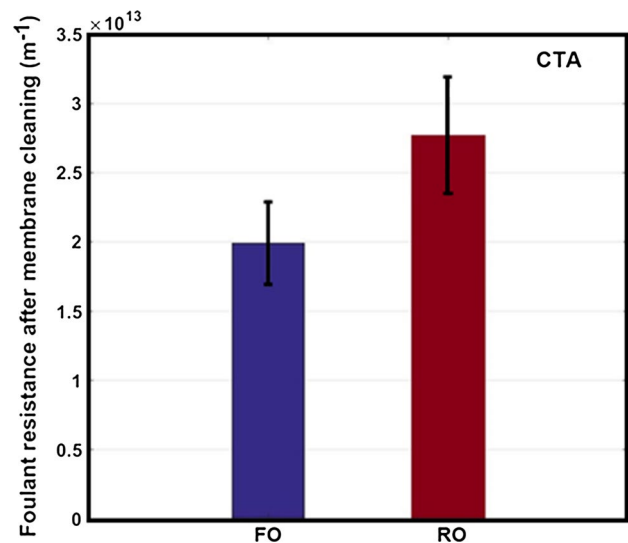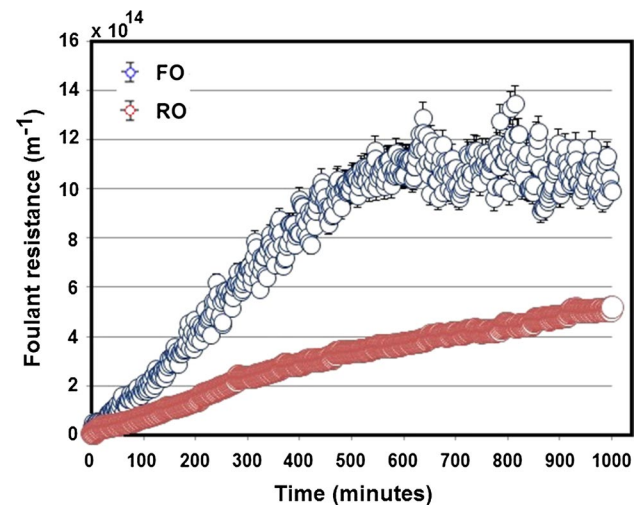
Fig. 10 Comparison of foulant resistance for FO and RO experiments using CTA membrane (ALFS orientation) with feed solution (45 mM NaCl + 5 mM CaCl$_2$) with alginate (200 mg/L) as foulant

The latter figure for RO accords with the value reported here. The value reported here for FO is significantly greater and a possible reason for this anomalous value has been given in Sect. 3.2. Given the findings in Fig. 7 (this work) and our earlier findings in [11], the true recovery values would not have been as dissimilar as shown here. This accords with the independently calculated value of foulant resistance after cleaning; see Fig. 9 taken from [31]. The resistance for FO is not approaching zero which it would if flux recovery had been close to 100%. This confirms the cautionary observation made in Sect. 3.2 regarding the reported flux recovery for alginate fouling of the TFC membrane after physical cleaning.

In [31], unlike [11] no allowance was made for cake-enhanced osmotic pressure but the resultant calculation of the time evolution of foulant resistance is strikingly similar in outline especially over the first 600 min. Overall these results confirm the overall headline message that FO acquires more foulant whilst ICP compensation ameliorates the flux decline (Fig. 10).

References

1. Cath TY, Childress AE, Elimelech M. Forward osmosis: Principles, applications, and recent developments. J Membr Sci. 2006;281:70–87.
2. Straub AP, Deshmukh A, Elimelech M. Pressure-retarded osmosis for power generation from salinity gradients: is it viable? Energy Environ Sci. 2016;9:31–48.
3. Wu JJ, Field RW. On the understanding and feasibility of "Breakthrough" Osmosis. Sci Rep. 2019;9:16464. https://doi.org/10.1038/s41598-019-53417-6.

4. http://www.powermag.com/statkraft-shelves-osmotic-power-project/ Accessed 3rd Nov 2021
5. Zhao S, Zou L, Tang CY, Mulcahy D. Recent developments in forward osmosis: opportunities and challenges. J Membr Sci. 2012;396:1–21.
6. Valladares Linares R, Li Z, Sarp S, Bucs S, Amy G, Vrouwenvelder JS. Forward osmosis niches in seawater desalination and wastewater reuse. Water Res. 2014;66:122–39.
7. Lutchmiah K, Verliefde ARD, Roest K, Rietveld LC, Cornelissen ER. Forward osmosis for application in wastewater treatment: a review. Water Res. 2014;58:179–97.
8. Wang X, Chang VWC, Tang CY. Osmotic membrane bioreactor (OMBR) technology for wastewater treatment and reclamation: advances, challenges, and prospects for the future. J Membr Sci. 2016;504:113–32.
9. Shaffer DL, Werber JR, Jaramillo H, Lin S, Elimelech M. Forward osmosis: where are we now? Desalination. 2015;356:271–84.
10. Chekli L, Phuntsho S, Kim JE, Kim J, Choi JY, Choi J-S, Kim S, Kim JH, Hong S, Sohn J, Shon HK. A comprehensive review of hybrid forward osmosis systems: performance, applications and future prospects. J Membr Sci. 2016;497:430–49.
11. Siddiqui FS, She Q, Fane AG, Field RW. Exploring the differences between forward osmosis and reverse osmosis fouling. J Membr Sci. 2018;565:241–53.
12. Chung T-S, Luo L, Wan CF, Cui Y, Amy G. What is next for forward osmosis (FO) and pressure retarded osmosis (PRO). Sep Purif Technol. 2015;156:856–60.
13. Lay WCL, Chong TH, Tang CY, Fane AG, Zhang J, Liu Y. Fouling propensity of forward osmosis: investigation of the slower flux decline phenomenon. Water Sci Technol. 2010;61:927–36.
14. Field RW, Pearce GK. Critical, sustainable and threshold fluxes for membrane filtration with water industry applications. Adv Colloid Interface Sci. 2011;164:38–44.
15. Jang Y, Cho H, Shin Y, Choi Y, Lee S, Koo J. Comparison of fouling propensity and physical cleaning effect in forward osmosis, reverse osmosis, and membrane distillation. Desalin Water Treat. 2016;57:24532–41.
16. Fane AG, Chong TH, Zhang J, Lay WLC, The effect of flux and pressure on fouling in reverse osmosis desalination, In: Proceedings IDA World Congress, Paper DB09-128; 2009.
17. Mi B, Elimelech M. Organic fouling of forward osmosis membranes: fouling reversibility and cleaning without chemical reagents. J Membr Sci. 2010;348:337–45.
18. Lee S, Boo C, Elimelech M, Hong S. Comparison of fouling behavior in forward osmosis (FO) and reverse osmosis (RO). J Membr Sci. 2010;365:34–9.
19. Kwan SE, Bar-Zeev E, Elimelech M. Biofouling in forward osmosis and reverse osmosis: measurements and mechanisms. J Membr Sci. 2015;493:703–8.
20. Xie Z, Nagaraja N, Skillman L, Li D, Ho G. Comparison of polysaccharide fouling in forward osmosis and reverse osmosis separations. Desalination. 2017;402:174–84.
21. McCutcheon JR, Elimelech M. Influence of concentrative and dilutive internal concentration polarization on flux behavior in forward osmosis. J Membr Sci. 2006;284:237–47.
22. Tang CY, She Q, Lay WCL, Wang R, Fane AG. Coupled effects of internal concentration polarization and fouling on flux behavior of forward osmosis membranes during humic acid filtration. J Membr Sci. 2010;354:123–33.
23. She Q, Wang R, Fane AG, Tang CY. Membrane fouling in osmotically driven membrane processes: a review. J Membr Sci. 2016;499:201–33.
24. Field RW, Wu JJ. On boundary layers and the attenuation of driving forces in forward osmosis and other membrane processes. Desalination. 2018;429:167–74.
25. Tow EW, Lienhard JH. Quantifying osmotic membrane fouling to enable comparisons across diverse processes. J Membr Sci. 2016;511:92–107.
26. She Q, Wong YKW, Zhao S, Tang CY. Organic fouling in pressure retarded osmosis: experiments, mechanisms and implications. J Membr Sci. 2013;428:181–9.
27. She Q, Hou D, Liu J, Tan KH, Tang CY. Effect of feed spacer induced membrane deformation on the performance of pressure retarded osmosis (PRO): implications for PRO process operation. J Membr Sci. 2013;445:170–82. https://doi.org/10.1016/j.memsci.2013.05.061.
28. Hoek EMV, Kim AS, Elimelech M. Influence of crossflow membrane filter geometry and shear rate on colloidal fouling in reverse osmosis and nanofiltration separations. Environ Eng Sci. 2002;19:357–72.
29. Field RW, Wu D, Howell J, Gupta JB. Critical flux concept for microfiltration fouling. J Membr Sci. 1995;100:259–72.
30. Nobel PS. The Boyle-van't Hoff relation. J Theoret Biol. 1969;23:375–9.
31. Siddiqui FA. Membrane filtration: fouling and cleaning in forward osmosis, reverse osmosis, and ultrafiltration membranes. D.Phil. thesis, Oxford; 2017.